Available online at www.sciencedirect.com
ScienceDirect
Journal of Magnetism and Magnetic Materials 320 (2008) 241–245
Journal of magnetism and magnetic materials
www.elsevier.com/locate/jmmm

Glass forming ability and magnetic properties of bulk metallic glasses $Fe_{68.7-x}C_{7.0}Si_{3.3}B_{5.5}P_{8.7}Cr_{2.3}Mo_{2.5}Al_{2.0}Co_x$ ($x = 0$–10)

H.X. Li, H.Y. Jung, S. Yi*

Department of Materials Science and Metallurgy, Kyungpook National University, Daegu 702-701, Korea

Received 10 April 2007; received in revised form 14 May 2007
Available online 5 June 2007

Abstract

Effects of partial substitutions of Co for Fe on the glass forming ability (GFA), mechanical and magnetic properties have been studied aiming at commercial magnetic and structural applications of bulk metallic glasses $Fe_{68.7-x}C_{7.0}Si_{3.3}B_{5.5}P_{8.7}Cr_{2.3}Mo_{2.5}Al_{2.0}Co_x$ ($x = 0$–10). Fully amorphous rods of 6 mm in diameter exhibiting fracture stress (σ_f) approaching 3.4 GPa and plastic strain (ε_p) of about 0.5% can be prepared through the replacement of 1–2 at% Fe by Co. Enhancement in GFA is attributed to the suppression of primary phase α-Fe with the optimum Co additions. Magnetic properties can be improved by the partial substitution of Co for Fe in the amount of 5 at% leading to the formation of amorphous ribbon with a saturation magnetization value of 0.85 T and a coercive force value of 11.5 A/m.

Keywords: Fe-based bulk metallic glass; Mechanical property; Magnetic property; Glass forming ability

1. Introduction

For soft magnetic applications, Fe-based metallic glasses have been commercialized in various alloy systems [1–4]. Due to lack of glass forming ability (GFA) of commercial Fe-based metallic glasses, however, manufacturing processes based upon rapid solidification ($>10^5$ K/s) have been required, limiting dimensions of the commercial Fe-based metallic glass materials to several tens of micrometers in thickness. Therefore, only functional applications of the commercial Fe-based metallic glasses have been considered using thin ribbons, fine powders or fibers [5–7]. Recently, some Fe-based bulk metallic glasses (BMGs) with relatively high GFA and attractive magnetic properties have been developed in the Fe-based multi-component systems including Fe-(Al,Ga)–(P,C,B,Si) [8–11], Fe–Mo–Ga–P–C–B–Si [12,13] and Fe–Mo–P–C–B–Si [14]. Since the Fe-based BMGs have high GFA, bulk soft magnetic materials with amorphous structure can be prepared through a relevant materials processing. However, even in the case of Fe-based BMGs mentioned above, extensive applications have been limited due to high production cost and low productivity of the Fe-based BMGs. That is, to secure high GFA of the Fe-based BMGs, high purity raw materials have to be used under a clean atmosphere during materials processing of the Fe-based BMGs. As a part of the program for the development of new BMGs for structural and functional applications, a series of Fe-based BMGs that can be produced cost-effectively in large quantities have been fabricated in the Fe–C–Si–B–P–Cr–Mo–Al alloy system [15–18]. In this study, partial replacements of Fe by Co that may be beneficial for magnetic properties of the Fe-based BMGs have been intended to improve magnetic properties. Magnetic properties, mechanical properties and GFA of the alloys $Fe_{68.7-x}C_{7.0}Si_{3.3}B_{5.5}P_{8.7}Cr_{2.3}Mo_{2.5}Al_{2.0}Co_x$ ($x = 0$–10) have been discussed.

2. Experimental procedure

Ingots with nominal compositions of $Fe_{68.7-x}C_{7.0}Si_{3.3}B_{5.5}P_{8.7}Cr_{2.3}Mo_{2.5}Al_{2.0}Co_x$ ($x = 0$–10 at%) were prepared by an arc melting process using industrial raw materials [17,18]. Rods with the diameter of up to 7 mm

*Corresponding author. Tel.: +82 53 950 5561; fax: +82 53 950 6559.
E-mail address: yish@knu.ac.kr (S. Yi).

0304-8853/$ - see front matter © 2007 Elsevier B.V. All rights reserved.
doi:10.1016/j.jmmm.2007.05.025

and the length of 50 mm were fabricated by a suction casting method using a copper mold with a cylindrical cavity of corresponding diameter. The splat ribbon samples with the thickness of 50–80 μm were prepared in a splat quencher. Phase analysis in as-cast or annealed samples was carried out using X-ray diffractometer (XRD) equipped with Cu target (CuK_α, $\lambda = 0.1541$ nm). The glass transition temperature, the onset temperature of crystallization event and liquidus temperature were measured by Differential Scanning Calorimetry (DSC) and Differential Thermal Analysis (DTA) at a heating rate of 40 and 20 K/min, respectively. Mechanical properties at room temperature were measured by Instron testing machine at a strain rate of 1.0×10^{-4}/s under a compression mode using amorphous rods ($\Phi 2 \times 4$ mm L). Magnetic properties including saturation magnetization (M_s) and coercive force (H_c) were measured with vibrating sample magnetometer (VSM) using a maximum field strength of 800 kA/m.

3. Results and discussion

3.1. Thermal and mechanical properties

The amorphous rods $Fe_{68.7-x}C_{7.0}Si_{3.3}B_{5.5}P_{8.7}Cr_{2.3}Mo_{2.5}Al_{2.0}Co_x$ ($x = 0$–10 at%) exhibit clear glass transition and multi-crystallization events during heating in DSC (Fig. 1). The amorphous structure of suction cast rods with various diameters were investigated through XRD and TEM analysis to determine the maximum diameter of fully amorphous rod according to compositional changes. As the maximum thickness of amorphous rod increases, the critical cooling rate for amorphous phase formation of the alloy tends to decrease, i.e., GFA of the alloy increases. Therefore, it can be concluded that the partial substitution of Fe by Co in the amount of 1 at% results in GFA enhancement of the alloy leading to the formation of fully amorphous rod of up to 6 mm in diameter. However, GFA of the alloys decreases with further substitution by Co. GFA of BMGs can often be estimated by parameters such as supercooled liquid region (ΔT_x), reduced glass transition temperature (T_{rg}) and γ value [19]. That is, higher GFA can be generally presumed as the parameter values increase. As can be inferred from Table 1, however, GFA of the alloys $Fe_{68.7-x}C_{7.0}Si_{3.3}B_{5.5}P_{8.7}Cr_{2.3}Mo_{2.5}Al_{2.0}Co_x$ seems not to be properly estimated by those parameters.

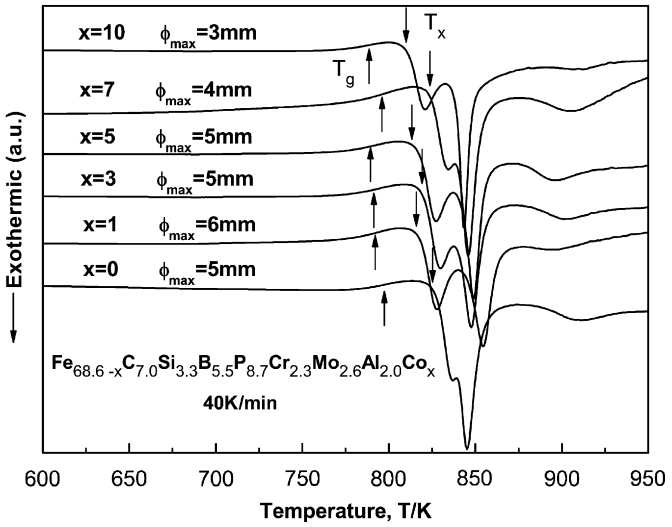

Fig. 1. The DSC heating traces of the fully amorphous rods with the maximum diameters of the $Fe_{68.7-x}C_{7.0}Si_{3.3}B_{5.5}P_{8.7}Cr_{2.3}Mo_{2.5}Al_{2.0}C_{ox}$ ($x = 0$, 1, 3, 5, 7, 10) alloys.

Fig. 2 shows XRD patterns of the suction cast rods $Fe_{68.7-x}C_{7.0}Si_{3.3}B_{5.5}P_{8.7}Cr_{2.3}Mo_{2.5}Al_{2.0}Co_x$ ($x = 0$, 1, 3). A broad halo pattern typical for amorphous phase can be obtained from the $\Phi 6$ rod containing 1 at% Co (Fig. 2b). Diffraction peaks overlapped the halo pattern were obtained from the $\Phi 6$ rods having the Co contents of 0 and 3 at%, revealing the existence of amorphous phase along with crystalline phases α-Fe, Fe_3C, Fe_2P and Fe_3B in the rods (Fig. 2a and e). It should be noted that $Fe_{23}C_6$ rather than α-Fe exists in the middle part of the $\Phi 7$ rod with 1 at% Co that was partially crystallized upon solidification (Fig. 2c). Meanwhile, existence of the same crystalline phases including α-Fe as those in the rods with the Co contents of 0 and 3 at% can be identified from the XRD pattern obtained from the top part of the $\Phi 7$ rod with 1 at% Co (Fig. 2d). Since the top part of a suction cast rod locates near melt pool, the cooling rate at the top part of a suction cast rod is generally lower than that at the middle part of the rod. Therefore, the top part of the $\Phi 7$ rod with 1 at% Co was fully crystallized into equilibrium phases, while a mixture of amorphous phase and crystalline phases were observed in the middle part of the $\Phi 7$ rod. Consequently, it can be inferred from the XRD patterns that the metastable $Fe_{23}C_6$ phase is formed first and then, transformed to the stable α-Fe phase during solidification of the $\Phi 7$ rod with 1 at% Co, while the stable α-Fe phase is directly formed from liquid upon cooling in the rods with the Co contents of 0 and 3 at%.

Fig. 3 shows the XRD patterns of amorphous rods with 0–3 at% Co annealed just below T_g for 1 h. It can be identified from the XRD patterns that the metastable $Fe_{23}C_6$ phase is formed first during devitrification of the amorphous rod with 1 or 2 at% Co (Fig. 3(b) and (c)), while precipitation of stable α-Fe phase direct from amorphous phase occurs in the rod with 0 or 3 at% Co (Fig. 3(a) and (d)).Based upon the experimental results during solidification and devitrification, it is concluded that optimum amounts of Co addition can suppress the formation of primary α-Fe phase leading to the formation of metastable $Fe_{23}C_6$ phase upon solidification. Fig. 4 shows the maximum diameter of fully amorphous rod as a function of Co contents for the $Fe_{68.7-x}C_{7.0}Si_{3.3}B_{5.5}P_{8.7}Cr_{2.3}Mo_{2.5}Al_{2.0}Co_x$ alloys. Minor addition of Co, i.e., 1 or 2 at%, is very effective to increase GFA, while a large amount of Co addition can dramatically decrease GFA. Therefore, enhanced GFA of the alloy with optimum amounts of Co may be the result of the precipitation of $Fe_{23}C_6$ phase while suppressing primary